



Synthesis and performance of a novel nanofiltration membrane with a crosslinked sulfonated polysulfone separation layer

Xiaoli Ding^{a,b,*}, Zhiguang Liu^c, Xu Li^{a,b}, Hongyong Zhao^{a,d}, Mingming Hua^{a,b},
Yuzhong Zhang^{a,b,*}

^aState Key Laboratory of Separation Membranes and Membrane Processes, Tianjin Polytechnic University, Tianjin 300387, China, emails: Dingxiaoli@tjpu.edu.cn (X. Ding), sdbzlx@163.com (X. Li), Zhaohongyong@tjpu.edu.cn (H. Zhao), 1531265767@qq.com (M. Hua), zhangyz2004cn@163.com (Y. Zhang)

^bInstitute of Separation Material and Process Control, School of Material Science and Engineering, Tianjin Polytechnic University, Tianjin 300387, China

^cCNOOC EnerTech-Drilling & Production Co., Tianjin 300452, China, email: 492177823@qq.com

^dSchool of Environmental and Chemical Engineering, Tianjin Polytechnic University, Tianjin 300387, China

Received 17 November 2015; Accepted 17 February 2016

ABSTRACT

The composite nanofiltration membrane was prepared by coating the covalent crosslinked sulfonated polysulfone on porous substrate. Polyethylene glycol (PEG), dopamine (DA) and *m*-phenylenediamine (MPD) were used as crosslinkers, respectively. The polyethersulfone/sulfonated polysulfone substrate was prepared by phase inversion. The membrane surface chemistry, hydrophilicity, morphology, PWF and rejections of PEG, methyl red and Na₂SO₄ were characterized. The effects of different crosslinkers and their concentrations on membrane characteristics were investigated. The effect of the sulfonated polysulfone concentration on the membrane characteristic was also investigated. The PEG crosslinked membrane showed the lowest contact angle of 9.0°, the highest PEG-600 rejection of 99.8%, the highest methyl red rejection of 99.8%, and the rejection of Na₂SO₄ was 93.4% and the PWF was 3.1 L m⁻² h⁻¹. The DA crosslinked membrane had the highest PWF of 51.5 L m⁻² h⁻¹, and the rejections of PEG-600, methyl red and Na₂SO₄ were 46.0, 44.0, and 34.0%, respectively. The MPD crosslinked membrane had the lowest PWF and rejections.

Keywords: Composite membrane; Nanofiltration; Crosslinked sulfonated polysulfone

1. Introduction

Water pollution is an urgent worldwide problem, and there are lots of technologies developed to obtain secure and sustainable source of water. Membrane technology has been applied in large-scale in water and wastewater treatment with the advantage of

strong adaptability, low operation pressure and low investment, etc. Nanofiltration (NF) has been also rapidly developed in the last decade for various industries, such as food and textile industry [1–3]. NF membranes are mainly made from cellulose acetate, cellulose triacetate, polyamide aromatic and sulfonated polyethersulfone (SPES), etc. Polysulfone (PSf) is also used in NF membrane fabrication with

*Corresponding authors.

the advantage of excellent mechanical, biological, chemical, and thermal stability. However, its relatively hydrophobic nature is a considerable limitation in water and wastewater treatment application because it is prone to high degree of fouling.

It is commonly accepted that the increase of membrane hydrophilicity offers better antifouling performance because protein and many other pollutants are hydrophobic in nature. Many works, which focused on the membrane antifouling, have been conducted by surface hydrophilic modification including surface coating and surface grafting [4,5]. And hydrophilicity of membrane material can be modified by blending with hydrophilic polymers [6,7] and nanoparticles [8–10], grafting with hydrophilic monomers like acrylic acid and acrylamide [11,12], sulfonation and amination [13–15], etc. Sulfonation has attracted great interest and sulfonated polysulfone (SPSf) and SPES have been used to fabricate the separation membrane for NF [16–20]. Our group also developed the polyethersulfone (PES)/SPSf blend nanofiltration membrane [21]. However, SPSf and SPES with high degree of sulfonation (DS) have poor mechanical stability because of high water swelling, which prevents the application in water and wastewater treatment. In order to overcome the swelling problem, Nohet et al. [22] prepared the crosslinking SPES membrane by reacting activated sulfonic acid with diamine. The result showed 50% reduction in swelling compared with noncrosslinked membranes. Tripathi et al. [23] also prepared the crosslinked SPES membrane for ultrafiltration by reacting activated sulfonic acid with poly(ethyleneglycol) bis-(3-aminopropyl) terminated, which resulted in the increase of the hydrophilicity and water flux. The crosslinking of highly sulfonated PSf has also been performed mainly for the proton conducting membrane [24].

The main objective of the study is to present a novel NF composite membrane fabricated by coating a crosslinked SPSf skin on the PES/SPSf membrane substrate. The separation layers were prepared by crosslinking SPSf with *m*-phenylenediamine (MPD), polyethylene glycol (PEG, $M_w = 200$) and dopamine (DA), respectively. The porous substrate was prepared by using PES/SPSf blending to increase the hydrophilicity of the supporting layer. In addition, the SPSf in supporting layers could crosslink with the crosslinker in the separation layer, which could strengthen the conjunction of the two layers. The membrane characterizations such as hydrophilicity, permeability and rejection, were investigated for membranes prepared in different conditions.

2. Experimental

2.1. Materials

SPSf (DS = 10 and 50%) were obtained from Tianjin Normal University, China. PES (Ultrason[®] E3010) was purchased from BASF. Polyvinylpyrrolidone (PVP, $M_w = 30,000$) was purchased from Shanghai Sunpower New Material Co., Ltd, China. PEG, MPD, and sodium sulfate (Na_2SO_4) were purchased from Tianjin Guangxia Fine Chemical Research Institute, China. DA was purchased from Wuhan Kangbao Fine Chemical Co., Ltd, China. *N,N*-dimethylacetamide (DMAC) and isopropanol were purchased from Tianjin Yingdaxigui Chemical Reagent Plant, China. Methyl red was purchased from Shanghai Hushi Laboratory Equipment Co., Ltd, China. All chemicals were used as received. Deionized water used in experiment was self-made in laboratory.

2.2. Fabrication of the composite membrane

2.2.1. The PES/SPSf substrate fabrication

The PES/SPSf porous membrane used as substrate was prepared by the Loeb–Sourirajan wet-phase inversion method. The casting solution was consisted of 12.6 wt% PES, 8.4 wt% SPSf (DS = 10%), 7 wt% PVP and 72 wt% DMAC. The casting solution was cast on the nonwoven fabric which is fixed on a flat glass plate by adhesive tape and then immersed into deionized water to form a porous substrate with a thickness of about 200 μm . After being peeled off from the glass plate, the membrane was washed in running water for 48 h to remove the residual solvent. And then the membrane was dried in nature air.

2.2.2. The composite membrane fabrication

The composite membrane was synthesized by coating method. SPSf (DS = 50%) was dissolved in the mixture of isopropanol and deionized water to form the homogeneous solution and then the crosslinker was added into the SPSf solution to form the coating solution. After being degassed, the coating solution was poured onto the substrate membrane, pressure was applied to the casting ring to prevent the solution from leaking. After 1 min, the coating solution was removed from the substrate membrane, and then, the membrane was suspended in a vacuum oven at 80°C for 2 h to allow the crosslinking reaction. The reaction schemes are presented in Fig. 1.

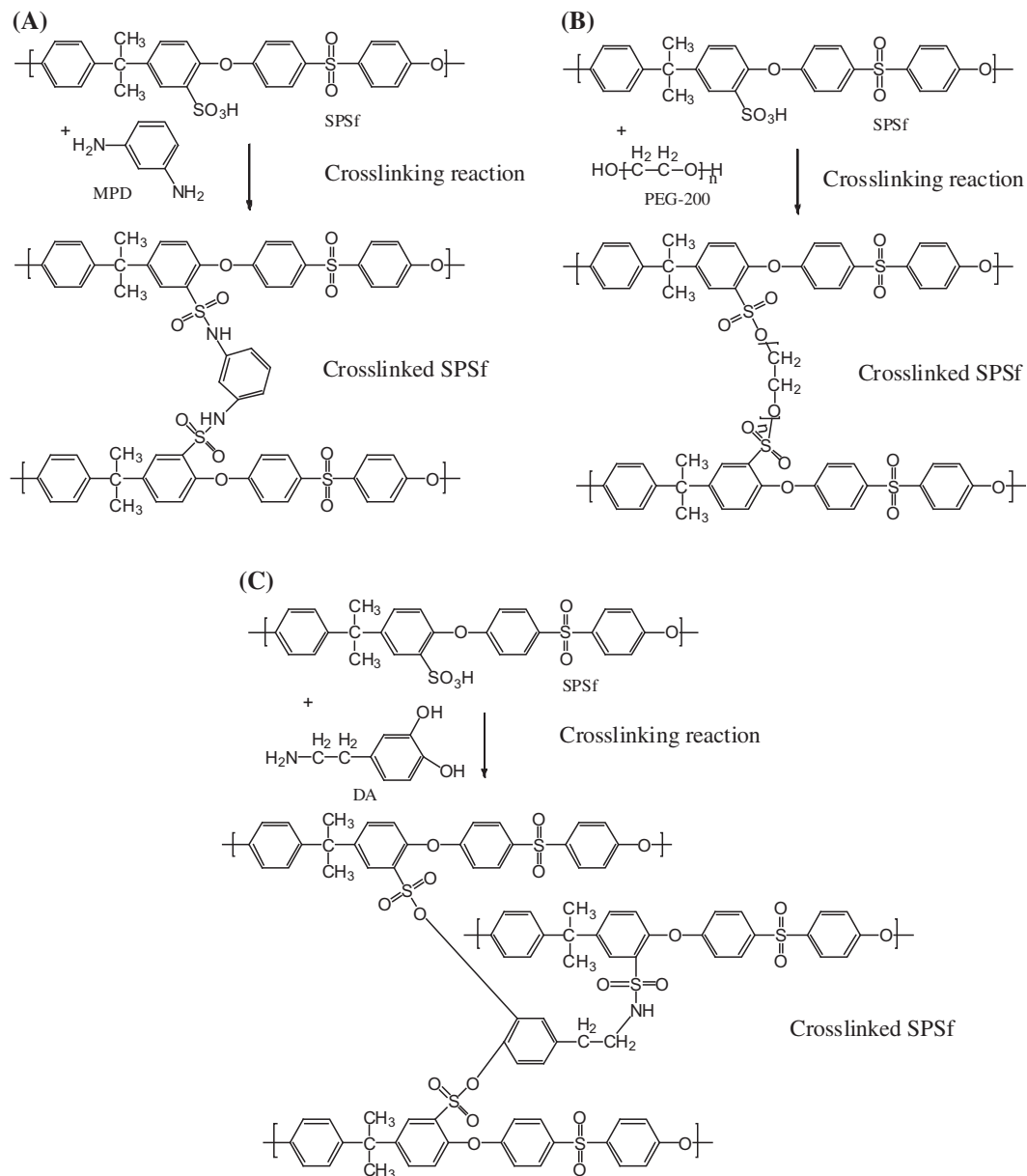


Fig. 1. Schemes for SPSf crosslinking reactions: (A) MPD crosslinked, (B) PEG crosslinked, and (C) DA crosslinked.

2.3. Characterization of the composite membrane

2.3.1. Chemical structure of the crosslinked coated layer

X-ray photoelectron spectroscopy (XPS, K-alpha X, Thermo Fisher, USA) was used to characterize the surface elemental content of membrane with a monochromatic Al $K\alpha_{1,2}$ X-ray source (15 kV, 150 W). The surface elemental stoichiometries were determined from peak area ratios after correcting with experimentally determined instrumental sensitivity factors. Attenuated total reflectance Fourier transform infrared spectroscopy (ATR-FTIR, Bruker Vector 22, Germany)

was used to characterize the chemical structure of membrane. For each measurement, 128 spectra were accumulated from 600 to 4,000 cm^{-1} at a resolution of 4 cm^{-1} .

2.3.2. Morphology of composite membrane

SEM of the membranes obtained by using a scanning electron microscope (SEM, Hitachi-s-4800, Japan) characterized the membrane surface and cross-section morphologies. One specimen was prepared for each case. The membrane specimen dried by a freeze dryer

(DF-1A-50, Beijing Boyikang, China) was fractured by using a sharp razor blade before sputtering with gold.

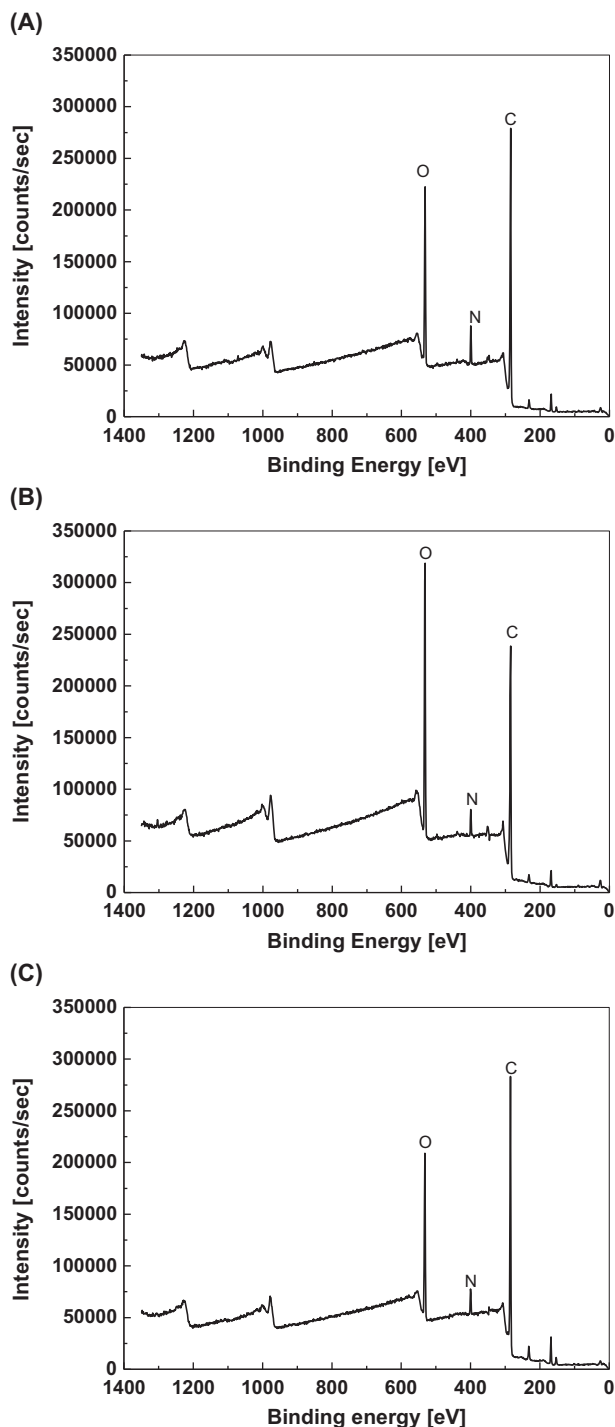


Fig. 2. XPS survey scan spectra of separation layers: (A) MPD crosslinked, (B) PEG crosslinked, and (C) DA crosslinked.

Table 1
Surface elemental composition (mol%) of oxygen, nitrogen, and carbon measured by XPS

Membrane	Surface elemental composition (mol%)		
	C	O	N
MPD crosslinked	71.6	18.1	6.0
PEG-200 crosslinked	64.0	28.6	3.8
DA crosslinked	72.0	20.1	4.0

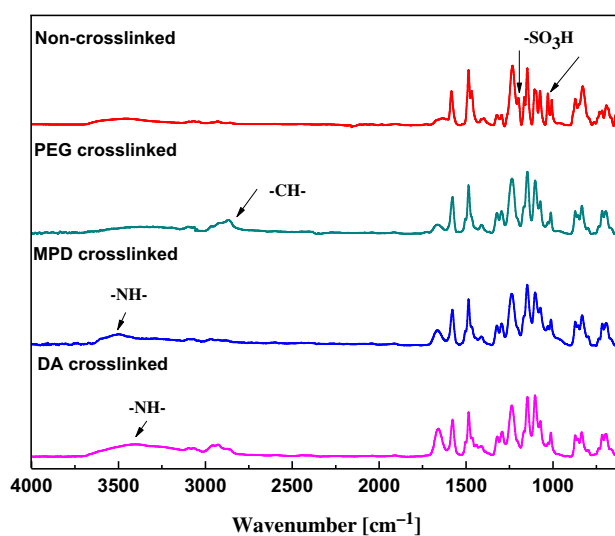


Fig. 3. ATR-FTIR spectra for the crosslinked skins of the composite membranes and noncrosslinked SPSf.

2.3.3. Hydrophilicity of the membrane surface

The surface hydrophilicity of the membrane was characterized by the static contact angle, which was evaluated by the sessile drop method in the contact angle goniometer (SL200KB, Shanghai Solon, China) using the deionized water as the probe liquid at room temperature. To minimize the experimental error, the contact angle was randomly measured at more than

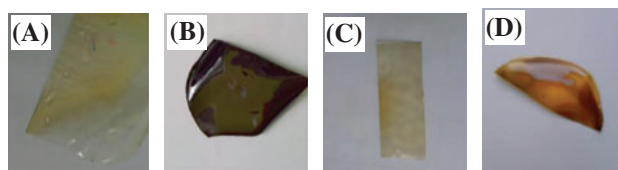


Fig. 4. The color changes of the membranes: (A) non-crosslinking, (B) MPD crosslinked, (C) PEG crosslinked, and (D) DA crosslinked.

five different locations for each specimen and the average value was reported.

2.3.4. NF performance of the composite membrane

NF performance of the composite membrane was tested by a laboratory-scale crossflow filtration unit at room temperature. The effective area of the membrane was 22.06 cm². Permeability data characterized by pure water flux (PWF, L m⁻² h⁻¹) was obtained by direct measurement of the permeate flow, which was calculated by the following equation [25]:

$$\text{PWF} = \frac{Q}{At} \quad (1)$$

where Q is the volume of permeate collected (L), A is the effective membrane surface area (m²) and t is the sampling time (h). The PWF was measured at 0.5 MPa after a compaction time of 30 min.

PEG ($M_w = 600$, PEG-600), dye (methyl red) and inorganic salt (Na₂SO₄), were used to determine the rejection of the composite membrane (R), which was calculated by the following equation [25]:

$$R (\%) = \left(1 - \frac{C_p}{C_f}\right) \times 100 \quad (2)$$

where C_p and C_f are the concentrations of the rejections in the permeate side and the feed side, respectively. The concentration of methyl red was determined by

measuring the absorbance at 433 nm with a UV–vis spectrophotometer (UV-2450, Shimadzu Co., Japan). The concentration of PEG-600 was determined by measuring the absorbance at 535 nm after iodine complexation [26]. The concentration of Na₂SO₄ was measured based on the conductivity measurement by the electrical conductivity (DDS-11A, Shanghai Hongyi Instrument Co., Ltd, China). The feed solutions were contained 1 g L⁻¹ Na₂SO₄, 1 g L⁻¹ PEG-600 and 0.1 g L⁻¹ methyl red, respectively.

3. Results and discussion

3.1. Chemical structure of the crosslinked separation layer

The XPS survey scans of the crosslinked separation skins are presented in Fig. 2. All membranes scanned were prepared in the same condition except the crosslinker. The intense signs of XPS peaks for C, O, and N elements appear in the spectra. The atomic concentration data from XPS analysis are presented in Table 1. The MPD crosslinked membrane had the lowest oxygen content and the highest nitrogen content caused by the highest molar percentage of nitrogen in MPD. The PEG-200 crosslinked membrane has the highest oxygen content caused by the highest molar percentage of oxygen in PEG-200. The results were expected according to the chemical compositions of the crosslinkers. Furthermore, the XPS results were qualitatively consistent with the ATR-FTIR results [23,27–29] and the color changes of the membranes (Figs. 3 and 4).

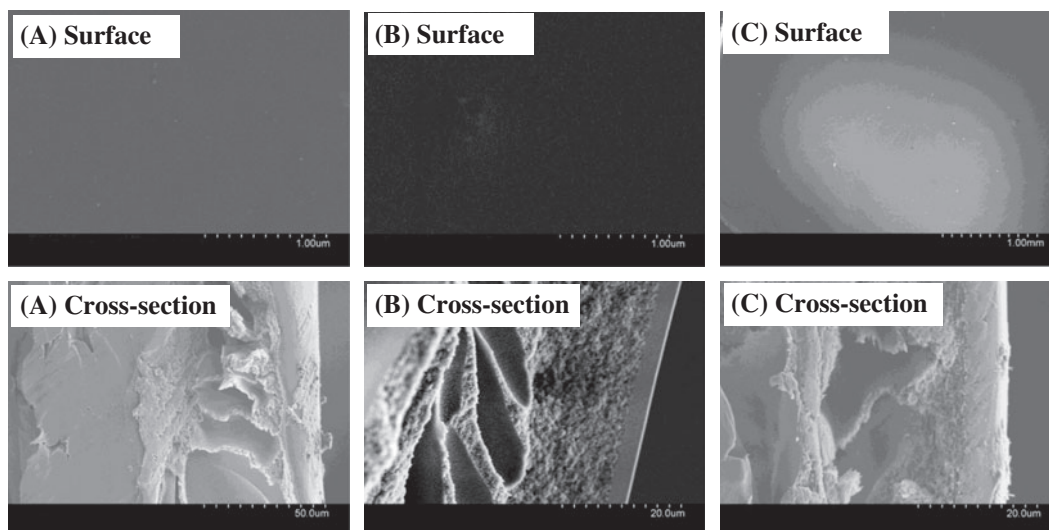


Fig. 5. Images of surface and cross-section morphologies: (A) MPD crosslinked, (B) PEG crosslinked, and (C) DA crosslinked.

3.2. Morphology of the composite membrane

The typical morphology of the composite membrane is depicted in Fig. 5. No significant difference was found except the thickness of the separation layer when the different crosslinkers were used. In the same condition, the membrane crosslinked with DA had the thickest separation layer, and the membrane crosslinked with PEG had the thinnest separation layer. The membrane surfaces were flat and smooth, no crack and big hole were observed. The cross-sectional image exhibited the typical asymmetric structure. The composite membrane was consisted of a dense symmetric skin and an asymmetric supporting layer. The supporting layer had a small portion of sponge-like structure beneath the top separation layer and finger-like cavities near the nonwoven fabric layer.

3.3. Hydrophilicity of the membrane surface

The contact angle is used to characterize the hydrophilicity of the membrane surface, which is presented in Figs. 6–8. The membrane skin crosslinked with MPD had the highest contact angle and some even exceeded 90° , which indicated the membrane skin was changed to be hydrophobic. The membrane skin crosslinked with DA had the lower contact angle than the membrane skin crosslinked with MPD, which mainly owed to the residual hydroxyl groups in skin since the crosslinker was excess. The membrane skin crosslinked with PEG had the lowest contact angle, which mainly owed to the hydrophilic PEG chain. The contact angles of membrane skins crosslinked with MPD and DA were independent of the concentrations of SPSf and the crosslinkers, while that of membrane

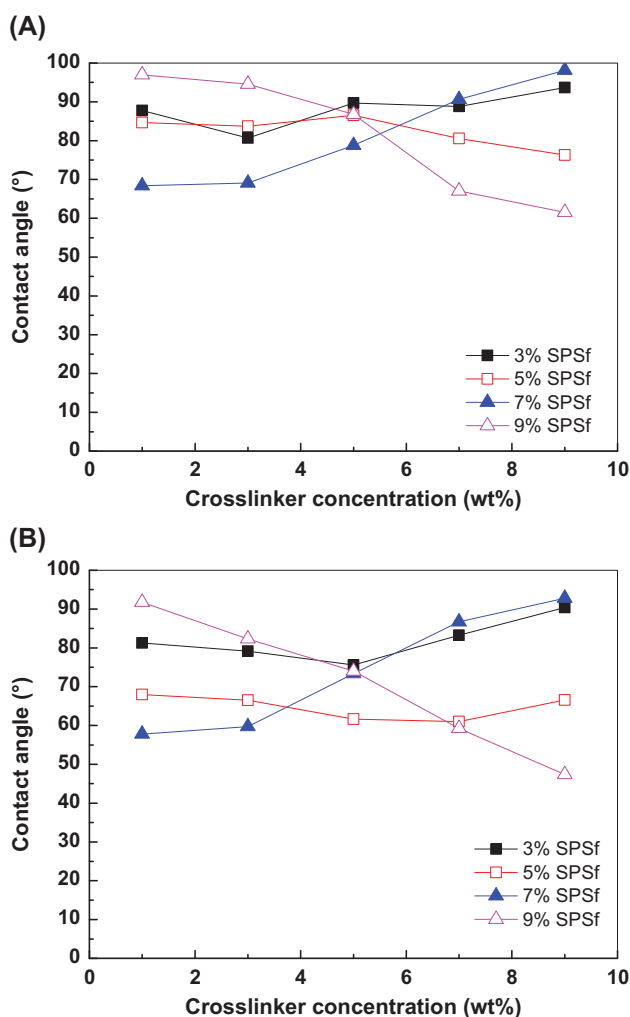


Fig. 6. Contact angles for composite membranes with MPD crosslinked skins: (A) tested at initial time and (B) tested after 30 s.

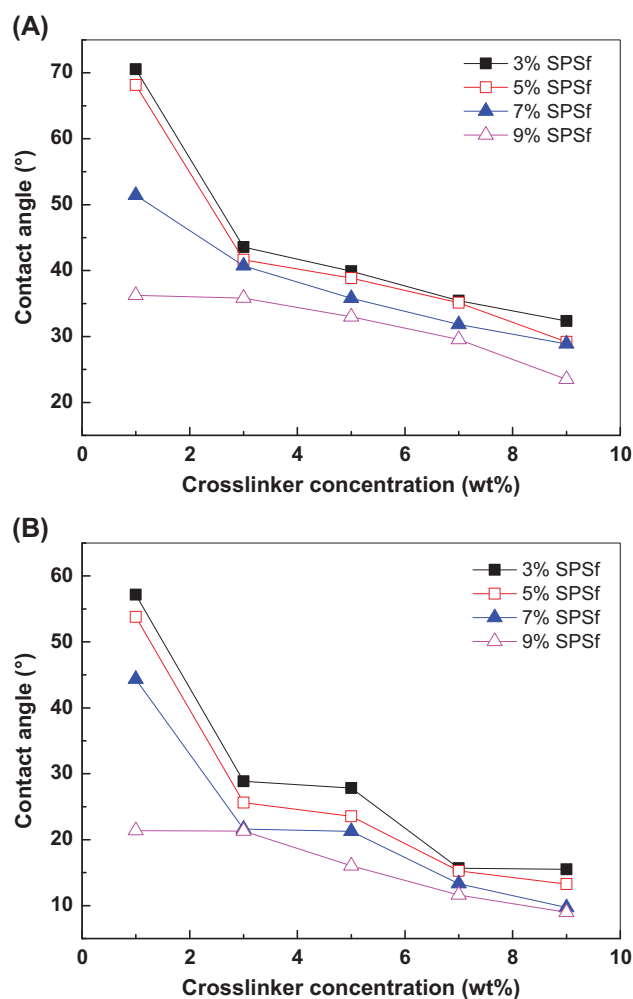


Fig. 7. Contact angles for composite membranes with PEG-200 crosslinked skins: (A) tested at initial time and (B) tested after 30 s.

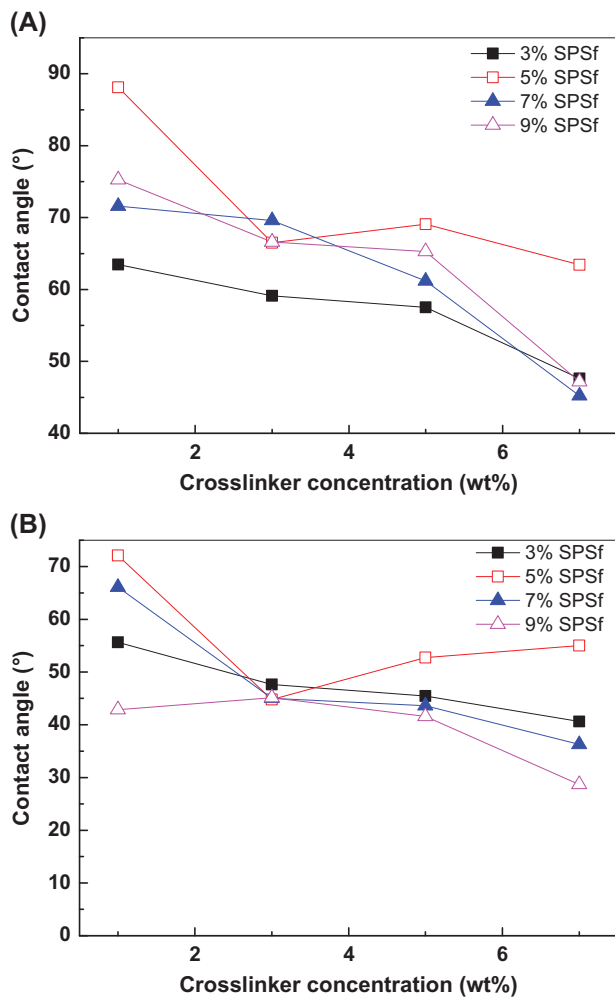


Fig. 8. Contact angles for composite membranes with DA crosslinked skins: (A) tested at initial time and (B) tested after 30 s.

skin crosslinked with PEG was decreased with the increase in concentrations of SPSf and the crosslinker. In Figs. 6–8, the time dependence is also presented by comparing the contact angle tested at initial time with which tested after 30 s. Water droplet volumes on the MPD crosslinked membrane were found to change insignificantly showed in Fig. 9(A) and (B), which also indicated that the effect of evaporation on the droplet volume could be neglected. Water droplet volumes on the PEG and DA crosslinked membranes were found to decrease showed in Fig. 9(C)–(F). The only reason for the decrease in water droplet volume could be due to the adsorption of the water by the hydrophilic skin, since the evaporation could be neglected [30].

3.4. Pure water flux and rejection of the composite membrane

The pure water flux and rejection of the composite membrane are presented in Figs. 10–13. The PWF was decreased with the increase in the crosslinker concentration and SPSf concentration (Fig. 10). The higher concentration of SPSf and crosslinker caused the higher crosslinking density and then the more compact coating layer. In addition, the higher crosslinking density induced the higher viscosity and then the thicker coating layer. The increases of compactness and thickness increased mass transfer resistance in membranes, which decreased the PWF. The membrane crosslinked with DA had the highest flux, while the membranes crosslinked with MPD had the lowest flux. The mass transfer resistance of the composite membrane is the sum of the mass transfer resistance of separation layer and supporting layer. At the same condition, the DA crosslinked solution had

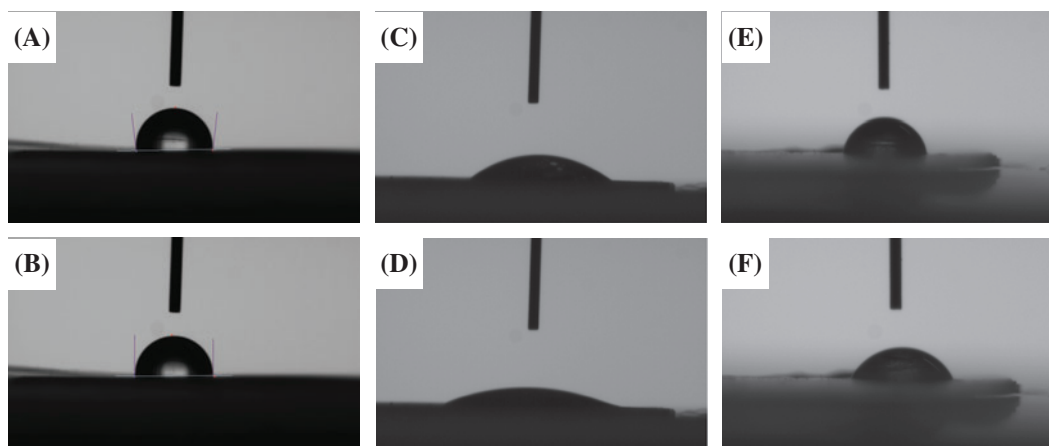


Fig. 9. Images of droplet corrected at initial time and after 30 s. (A) and (B) crosslinked with MPD; (C) and (D) crosslinked with PEG-200; (E) and (F) crosslinked with DA; (A), (C) and (E) corrected at initial time, (B), (D) and (F) corrected after 30 s. The concentration of SPSf was 1 wt% and the concentration of crosslinker was 9 wt%.

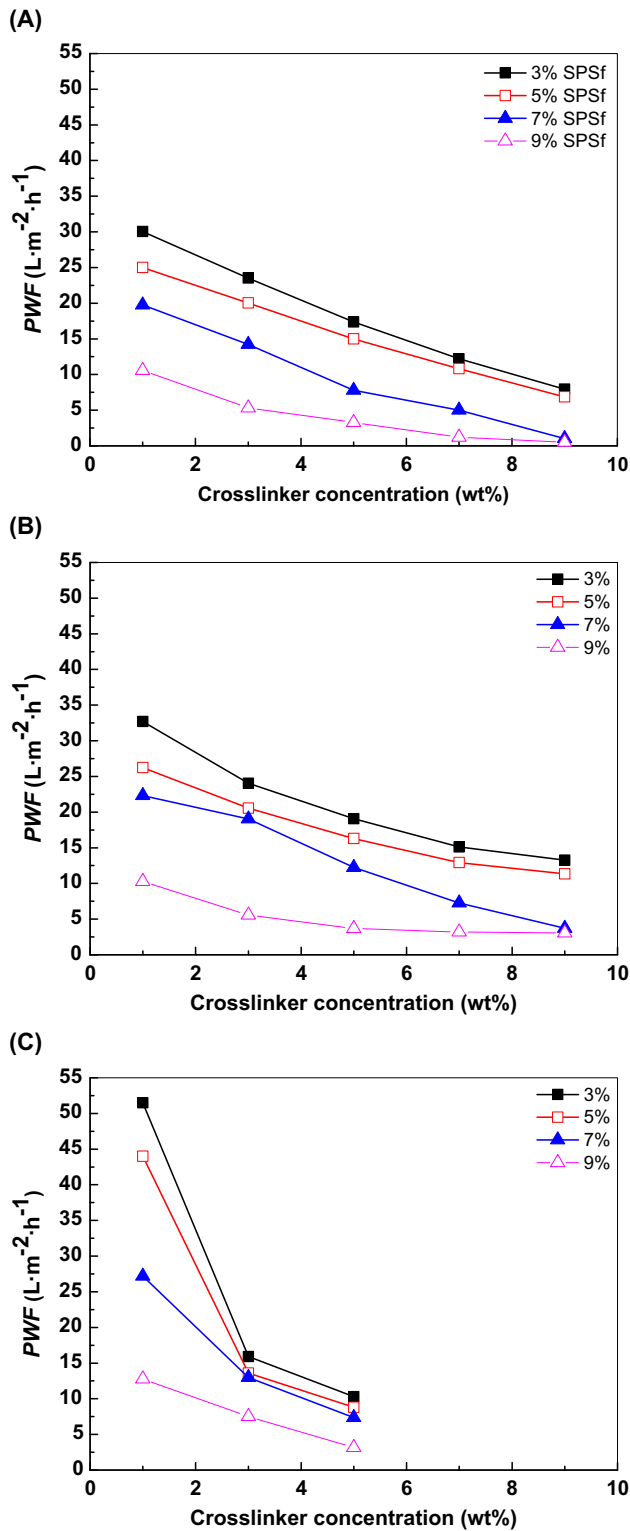


Fig. 10. Pure water flux of the composite membrane: (A) MPD crosslinked, (B) PEG crosslinked, and (C) DA crosslinked.

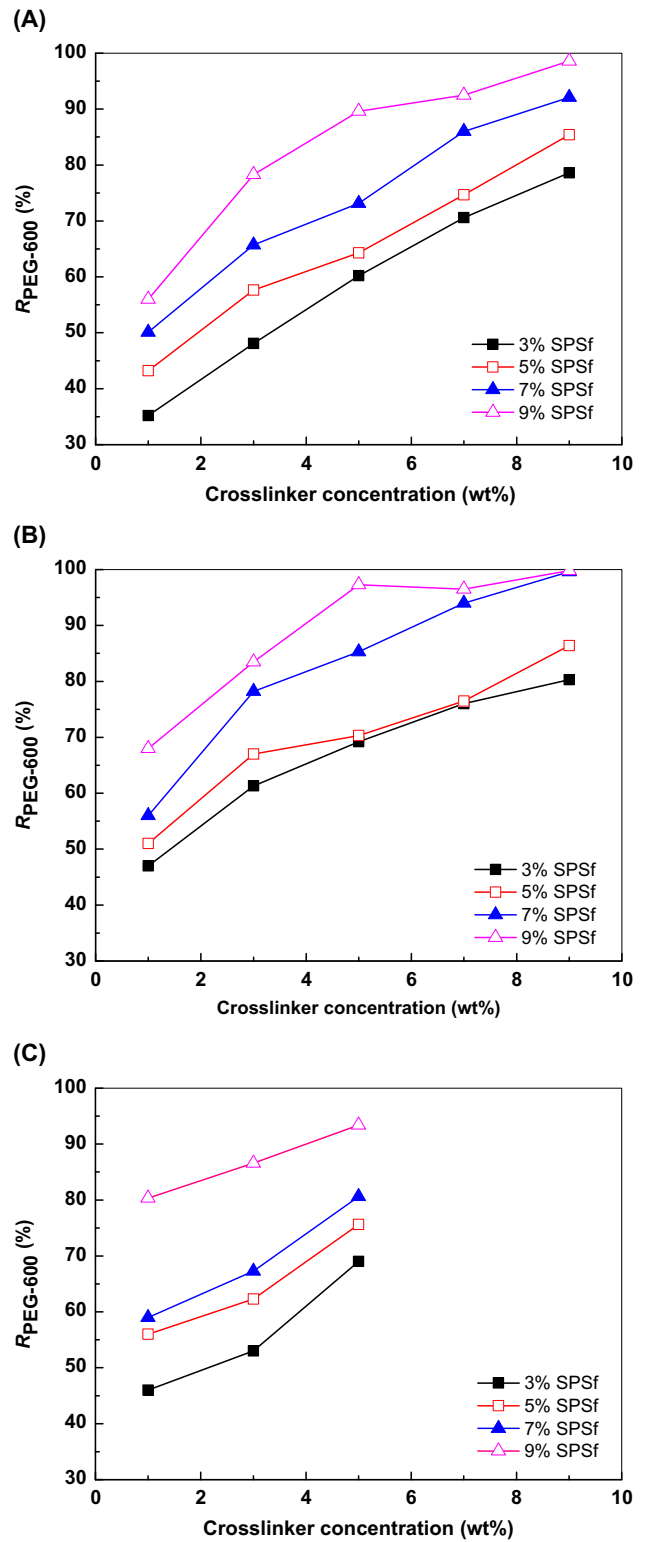


Fig. 11. PEG-600 rejection of the composite membrane: (A) MPD crosslinked, (B) PEG crosslinked, and (C) DA crosslinked.

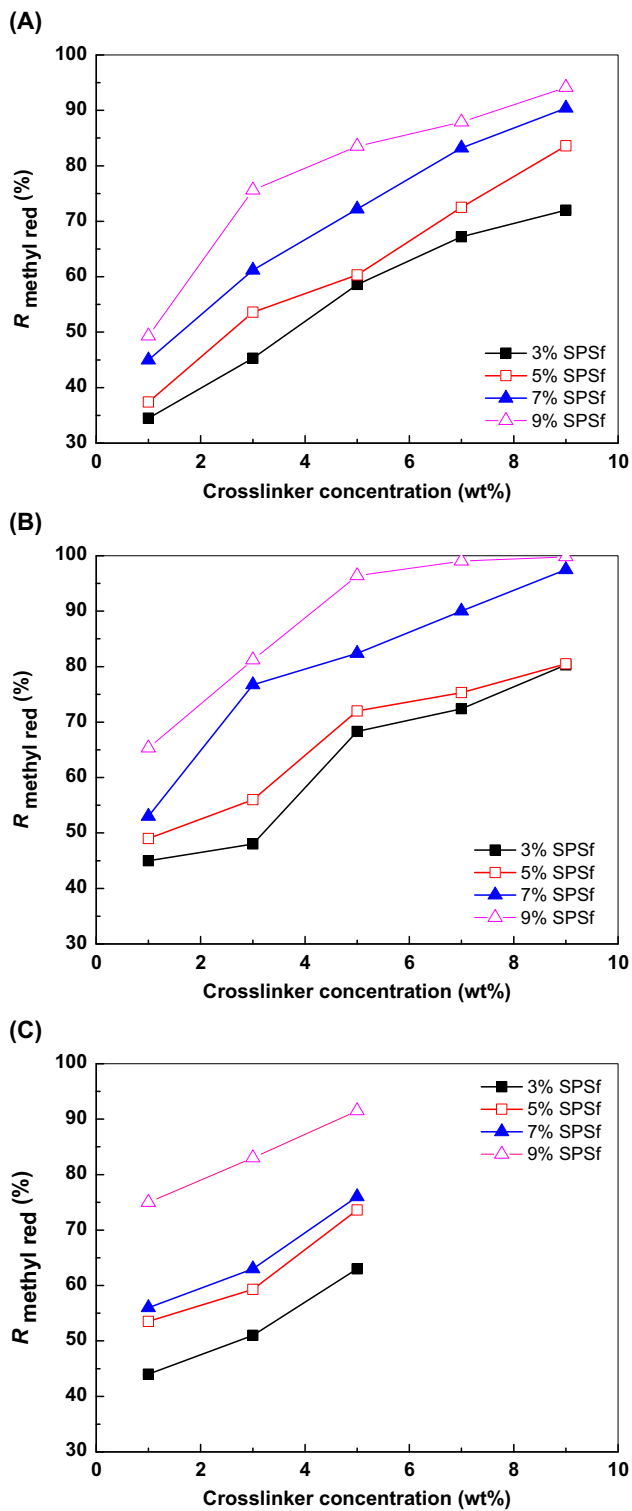


Fig. 12. Methyl red rejection of the composite membrane: (A) MPD crosslinked, (B) PEG crosslinked, and (C) DA crosslinked.

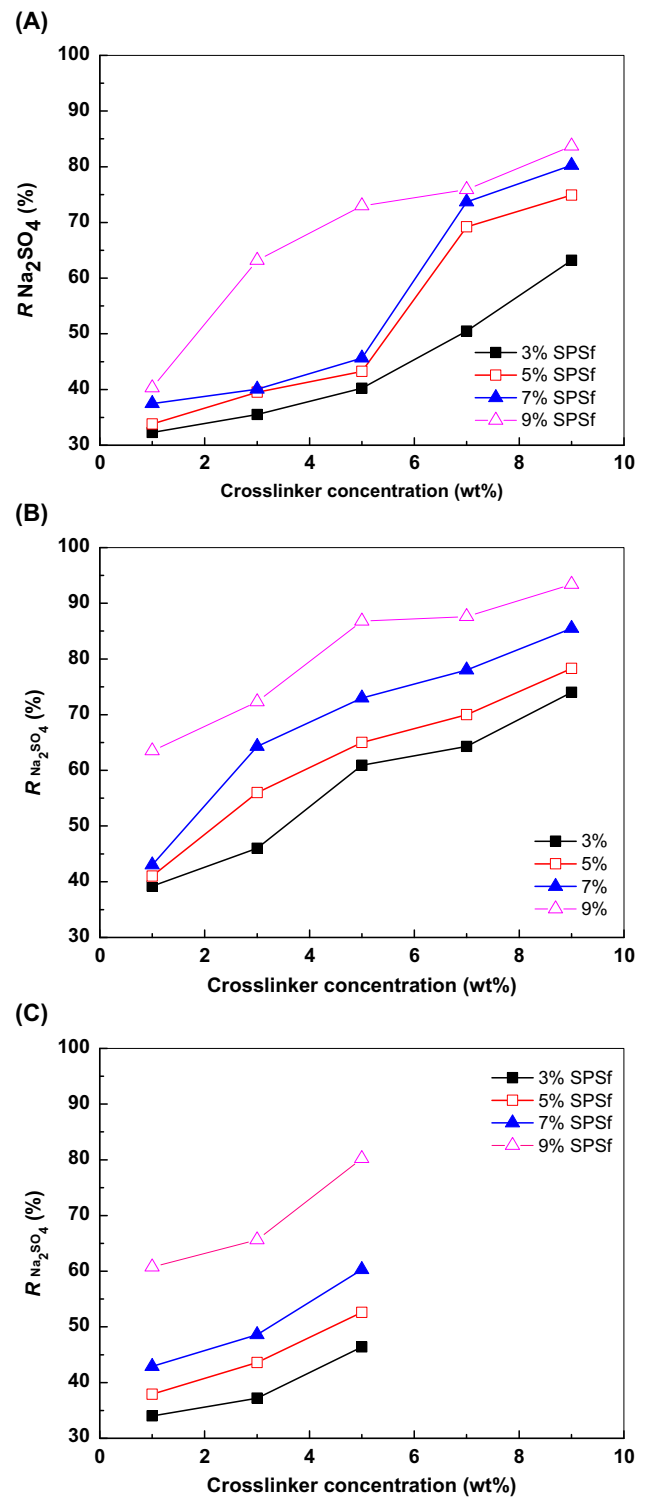


Fig. 13. Na_2SO_4 rejection of the composite membrane: (A) MPD crosslinked, (B) PEG crosslinked, and (C) DA crosslinked.

the highest crosslinking density due to three functional groups in one DA molecule. The higher crosslinking density induced higher viscosity, which induced the less intrusion of the coating solution into the supporting layer. The intrusion of coating solution increased the mass transfer resistance and decreased the PWF. This phenomenon has been widely studied in the composite membrane for gas separation synthesized by coating method [31,32] and also appeared in this study. Both MPD molecule and PEG-200 molecule have two functional groups, while MPD has smaller molecular weight than PEG-200. With the same concentration, the MPD crosslinked solution had the higher crosslinking density than the PEG-200 crosslinked solution. As described above, the higher crosslinking density induced the more compact skin of membrane. The compact structure increased the mass transfer resistance of the membrane and then decreased the PWF. On the other hand, the membrane crosslinked with PEG-200 had more hydrophilic skin contributed by ether oxygen groups, which increased the PWF. The membranes crosslinked with PEG-200 had the higher fluxes than membranes crosslinked with MPD.

The rejections of the membranes were increased with the increase of SPSf concentration and crosslinker concentration (Figs. 11–13). The increase in the SPSf and crosslinker concentration induced the increase in the crosslinking density, and then, the structure compactness, which decreased the PWF and increased the rejection. The membrane with a skin crosslinked with 9 wt% SPSf and 9 wt% PEG-200, had the highest separation performance with a PEG-600 rejection of 99.8%, methyl red rejection of 99.8%, Na_2SO_4 rejection of 93.4%. In all membranes, the PEG-600 rejection had the highest values, while the Na_2SO_4 rejection had the lowest values, since the PEG-600 has the highest molecule weight and largest molecular size. For PEG-600 rejection and methyl red rejection, the membranes crosslinked with DA had the highest values since the most compact structure in the membrane skin due to the highest crosslinking density. The membranes crosslinked with PEG-200 had the higher PEG-600 rejection and methyl red rejection due to the higher water flux, even the membranes crosslinked with MPD had the more compact and rigid structure in membrane skin due to higher crosslinking density and benzene ring. For Na_2SO_4 rejection, the membranes crosslinked with MPD had the lowest values, while the membranes crosslinked with PEG-200 had the highest values even with the loosest structure in membrane skins. H-bonds formed between the water and ether oxygen

groups in the skins of membranes crosslinked with PEG-200, and then, a layer of pure water formed at the interface of membrane–solution, which hinder the absorption and transfer of inorganic salt. The membrane crosslinked with DA had more compact and hydrophilic skin than the membrane crosslinked with MPD, and then had the higher Na_2SO_4 rejection.

4. Conclusion

NF series membranes with a crosslinked SPSf skin were prepared by coating method. The crosslinking changed the hydrophilic and hydrophobic characteristics of the membrane surface. The membrane with a PEG crosslinked skin had a hydrophilic surface with a lowest contact angle of 9.0° , and the contact angle decreased with the increase in the concentration of SPSf and PEG. While the membrane with a MPD crosslinked skin had a hydrophobic surface with a contact angle of 96.9° , the membrane with a DA crosslinked skin had a more hydrophilic skin than the membrane crosslinked with MPD due to the residual hydroxy group. The contact angle was independent of the concentration of SPSf, MPD and DA. The flux and rejections had closed correlations with the concentration of crosslinker, the concentration of SPSf and the surface hydrophilicity. The membrane with a DA crosslinked skin had a highest pure water flux, methyl red rejection, and PEG-600 rejection. The membrane with a MPD crosslinked skin had a lowest pure water flux and rejections for all analytes. The membrane with a PEG crosslinked skin had a highest Na_2SO_4 rejection.

Acknowledgments

The authors wish to sincerely thank the National Natural Science Foundation of China (Grant No. 21206121, 51373120, 51173132, 21274108, 21506160), Tianjin City High School Science & Technology Fund Planning Project (Grant No. 20090514), Tianjin Research Program of Application Foundation and Advanced Technology (Grant No. 14JCQNJC06400), the Scientific Research Foundation for the Returned Overseas Chinese Scholars, State Education Ministry (No. 48), Tianjin Training Program of Innovation and Entrepreneurship for Undergraduates (Grant No. 201510058067) and State Key Laboratory of Separation Membranes and Membrane Processes (Tianjin Polytechnic University) Fund Program (Grant No. Z2-201508, Z2-201565) for financially supporting this work.

References

- [1] T. Puspasari, N. Pradeep, K.-V. Peinemann, Cross-linked cellulose thin film composite nanofiltration membranes with zero salt rejection, *J. Membr. Sci.* 491 (2015) 132–137.
- [2] B. Yuzer, M.I. Aydin, F.B. Bulut, S. Palamutcu, U. Emer, M. Bekbolet, S. Pak, H. Selçuk, Reuse of the treated textile wastewater and membrane brine in the wet textile processes: Distorting effects on the cotton fabric, *Desalin. Water Treat.* 56 (2015) 997–1009.
- [3] D. Zhou, L. Zhu, Y. Fu, M. Zhu, L. Xue, Development of lower cost seawater desalination processes using nanofiltration technologies—A review, *Desalination* 376 (2015) 109–116.
- [4] E.M. Van Wagner, A.C. Sagle, M.M. Sharma, Y.H. La, B.D. Freeman, Surface modification of commercial polyamide desalination membranes using poly(ethylene glycol) diglycidyl ether to enhance membrane fouling resistance, *J. Membr. Sci.* 367 (2011) 273–287.
- [5] B. Van der Bruggen, Chemical modification of polyethersulfone nanofiltration membranes: A review, *J. Appl. Polym. Sci.* 114 (2009) 630–642.
- [6] E. Eren, A. Sarihan, B. Eren, H. Gumus, F.O. Kocak, Preparation, characterization and performance enhancement of polysulfone ultrafiltration membrane using PBI as hydrophilic modifier, *J. Membr. Sci.* 475 (2015) 1–8.
- [7] A. Pagidi, R. Saranya, G. Arthanareeswaran, A.F. Ismail, T. Matsuura, Enhanced oil–water separation using polysulfone membranes modified with polymeric additives, *Desalination* 344 (2014) 280–288.
- [8] A. Sotto, A. Boromand, R. Zhang, P. Luis, J.M. Arsuaga, J. Kim, B. Van der Bruggen, Effect of nanoparticle aggregation at low concentrations of TiO₂ on the hydrophilicity, morphology, and fouling resistance of PES-TiO₂ membranes, *J. Colloid Interface Sci.* 363 (2011) 540–550.
- [9] V. Vatanpour, S.S. Madaeni, A.R. Khataee, E. Salehi, S. Zinadini, H.A. Monfared, TiO₂ embedded mixed matrix PES nanocomposite membranes: Influence of different sizes and types of nanoparticles on antifouling and performance, *Desalination* 292 (2012) 19–29.
- [10] A. El-Aassar, Improvement of reverse osmosis performance of polyamide thin-film composite membranes using TiO₂ nanoparticles, *Desalin. Water Treat.* 55 (2015) 2939–2950.
- [11] I. Gancarz, G. Poźniak, M. Bryjak, A. Frankiewicz, Modification of polysulfone membranes. 2. Plasma grafting and plasma polymerization of acrylic acid, *Acta Polym.* 50 (1999) 317–326.
- [12] J. Wang, H.J. Sun, X.L. Gao, C.J. Gao, Enhancing antibiofouling performance of Polysulfone (PSf) membrane by photo-grafting of capsaicin derivative and acrylic acid, *Appl. Surf. Sci.* 317 (2014) 210–219.
- [13] I. Yum, D. Jeong, J. Oh, Y. Lee, A novel sulfonated poly(arylene ether ketone) reverse osmosis membrane: Effect of casting condition on separation characteristics, *Desalin. Water Treat.* 17 (2010) 204–209.
- [14] R. Mahendran, P.K. Bhattacharya, Preparation and characterization of positively charged polysulfone nanofiltration membranes, *J. Polym. Eng.* 33 (2013) 369–376.
- [15] S.G. Kim, S.Y. Park, J.H. Chun, B.H. Chun, S.H. Kim, Novel thin-film composite membrane for seawater desalination with sulfonated poly(arylene ether sulfone) containing amino groups, *Desalin. Water Treat.* 43 (2012) 230–237.
- [16] B. Van der Bruggen, Comparison of redox initiated graft polymerisation and sulfonation for hydrophilisation of polyethersulfone nanofiltration membranes, *Eur. Polym. J.* 45 (2009) 1873–1882.
- [17] E.T.R. Bastos, C.C.R. Barbosa, J.C. Silva, V.B.C. Queiroz, D.S. Vaitsman, Development of sulfonated polysulfone composite membranes for ammonium rejection, *Membr. Water Treat.* 4 (2013) 83–93.
- [18] R. Chennamsetty, I. Escobar, X.L. Xu, Polymer evolution of a sulfonated polysulfone membrane as a function of ion beam irradiation fluence, *J. Membr. Sci.* 280 (2006) 253–260.
- [19] M. Padaki, A.M. Isloor, P. Wanichapichart, A.F. Ismail, Preparation and characterization of sulfonated polysulfone and N-phthloyl chitosan blend composite cation-exchange membrane for desalination, *Desalination* 298 (2012) 42–48.
- [20] A.K. Ghosh, V. Ramachandhran, M.S. Hanra, B.M. Misra, Synthesis, characterization, and performance of sulfonated polyethersulfone nanofiltration membranes, *J. Macromol. Sci., Part A* 39 (2002) 199–216.
- [21] F. Ma, H. Ye, Y.Z. Zhang, X.L. Ding, L.G. Lin, L.Z. Zhao, H. Li, The effect of polymer concentration and additives of cast solution on performance of polyethersulfone/sulfonated polysulfone blend nanofiltration membranes, *Desalin. Water Treat.* 52 (2014) 618–625.
- [22] R. Nolte, K. Ledjeff, M. Bauer, R. Mülhaupt, Partially sulfonated poly(arylene ether sulfone)-A versatile proton conducting membrane material for modern energy conversion technologies, *J. Membr. Sci.* 83 (1993) 211–220.
- [23] B.P. Tripathi, N.C. Dubey, M. Stamm, Polyethylene glycol cross-linked sulfonated polyethersulfone based filtration membranes with improved antifouling tendency, *J. Membr. Sci.* 453 (2014) 263–274.
- [24] S. Yuan, G.W. Yan, Z.J. Xia, X.X. Guo, J.H. Fang, X.H. Yang, Preparation and properties of covalently cross-linked sulfonated poly(sulfide sulfone)/polybenzimidazole blend membranes for fuel cell applications, *High Perform. Polym.* 26 (2014) 212–222.
- [25] Y.F. Li, Y.L. Su, J.Y. Li, X.T. Zhao, R.N. Zhang, X.C. Fan, J.A. Zhu, Y.Y. Ma, Y. Liu, Z.Y. Jiang, Preparation of thin film composite nanofiltration membrane with improved structural stability through the mediation of polydopamine, *J. Membr. Sci.* 476 (2015) 10–19.
- [26] A.D. Sabde, M.K. Trivedi, V. Ramachandhran, M.S. Hanra, B.M. Misra, Casting and characterization of cellulose acetate butyrate based UF membranes, *Desalination* 114 (1997) 223–232.
- [27] J.J. Yu, The Performance and Cross-Linking Character for Sulfonated Poly(bis-A)-sulfone Proton Exchange Membranes, Hubei University, Wuhan, 2009.
- [28] J.H. Hu, X.F. Z, Practical Infrared Spectroscopy, Science Press, Beijing, 2011.
- [29] H.Y. Zhao, Y.M. Cao, X.L. Ding, M.Q. Zhou, Q. Yuan, Effects of cross-linkers with different molecular weights in cross-linked Matrimid 5218 and test temperature

- on gas transport properties, *J. Membr. Sci.* 323 (2008) 176–184.
- [30] C.M. Weikart, M. Miyama, H.K. Yasuda, Surface modification of conventional polymers by depositing plasma polymers of trimethylsilane and of trimethylsilane + O₂, *J. Colloid Interface Sci.* 211 (1999) 18–27.
- [31] T.S. Chung, E.S.P. Loh, J.J. Shieh, A simple approach to estimate gas permeability and selectivity of extremely thin and brittle materials, *Chem. Eng. Sci.* 55 (2000) 1093–1099.
- [32] X.L. Ding, C. Zhang, Y.Z. Zhang, Z.P. Cao, Fabrication of PEBAX 2533/PSf hollow fiber composition membrane and its transfer resistance, *Chem. J. Chin. Univ.* 33 (2012) 2591–2596.